Spectroscopic and Dynamic Studies of the Epidermal Chromophores *trans*-Urocanic Acid and Eumelanin

JOHN D. SIMON

Department of Chemistry, Duke University, and Department of Biochemistry, Duke University Medical Center, Durham, North Carolina 27708

Received August 10, 1999

ABSTRACT

Photoaging and skin cancer can result from the exposure of skin to ultraviolet A (UV-A, 320−400 nm) radiation. The detailed chemical mechanisms by which these processes occur are not known, but they must begin with the absorption of a UV-A photon by one or more photoreceptor(s) within the skin. The situation is complicated by the lack of understanding of the photoreactions of many of the UV-A-absorbing molecules in skin. In this Account, we describe recent research efforts directed at elucidating the UV-A-induced photoreactivity of two light-absorbing epidermal photoreceptors: *trans*-urocanic acid and eumelanin.

Chronic exposure of the skin to ultraviolet radiation can cause premature aging and cancer. UV-A (320−400 nm)-photoaged skin is characterized by a variety of physiological changes including an increase in the elastic fibers (e.g., elastin) of the skin, which serves to replace the collagenated dermal matrix.[1−4] Although the mechanisms by which such UV-A-induced photodamage occurs have not been completely determined, there is strong evidence that reactive oxygen species play a role.[5] Specifically, exposure to UV radiation has been shown both to reduce the antioxidant population in the skin[6] and to sensitize the production of reactive oxygen species such as singlet oxygen, hydrogen peroxide, and the superoxide anion.[7,8] Formation of these latter species enables oxidation of lipids and proteins, which can affect the degree of cross-linking between collagen and other proteins.[9]

The photoaging of skin is not the only possible adverse result of excessive exposure to UV-A radiation. While significant attention has been paid to UV-B (280−320 nm) exposure (the region of direct DNA absorption), recent data indicate that UV-A radiation also plays an important role in the development of skin cancer.[10] The incidences of skin cancers (both melanoma and nonmelanoma) are increasing.[11] As with photoaging, the pathways by which UV-A induces cancers are believed to involve reactive oxygen species that are photochemically generated either directly or indirectly by a UV-A-absorbing molecule.[12]

Scheme 1[18]

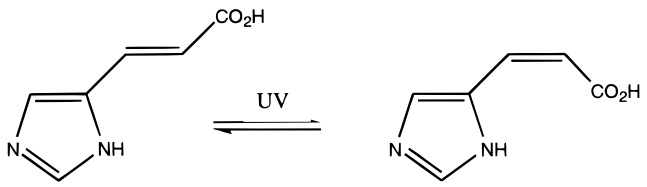

trans-urocanic acid cis-urocanic acid

In our work we have tried to characterize the photoreactions of UV-A photoreceptors in skin. We are especially interested in those molecules that can photochemically produce reactive oxygen species. In the Account that follows, we focus on two such molecular systems: *trans*-urocanic acid and eumelanin. One of the major goals of this research is to establish links between the in vitro photochemistry of these systems and the action spectra for in vitro and in vivo UV-induced responses in skin.

Urocanic Acid. The epidermal chromophore urocanic acid (UCA) has received considerable attention because of its immunomodulatory behavior.[13−15] UCA is synthesized as a trans isomer (*t*-UCA, approximately 30 μg/cm^2) in the uppermost layer of the skin (stratum corneum).[16] *t*-UCA accumulates in the epidermis until it is either removed by the monthly skin renewal cycle or dissolved in sweat.[17]

Upon absorption of UV light, *t*-UCA isomerizes to its cis form, *c*-UCA (Scheme 1), which has an absorption spectrum similar to that of *t*-UCA. *c*-UCA photoisomerizes back to the trans isomer, and thus a photostationary state between the two isomers is ultimately attained.[19] Because DNA lesions (e.g., pyrimidine dimers) in the lower epidermis can result from UV-B absorption, initial research proposed that *t*-UCA acts as a natural sunscreen.[20] In 1983, Drs. Ed De Fabo and Frances Noonan showed that the action spectrum for immune suppression of contact hypersensitivity overlapped the absorption spectrum of *t*-UCA.[13] Building upon this observation, they proposed that *c*-UCA depresses the immune system in skin. Since then, researchers have found that *c*-UCA induces a variety of biological responses.[21−25] An excellent review article on the photobiology of UCA was recently published by Mohammad, Morrison, and HogenEsch.[26]

Wavelength-Dependent Photochemistry of *t*-UCA. *t*-UCA is an unusual molecule because the photoisomerization quantum yield is wavelength-dependent.[27] The photoisomerization efficiency (Φ) peaks at 310 nm (the red edge of the absorption spectrum) with $\Phi = 0.49$, and is reduced near the absorption maximum (at 266 nm) with $\Phi = 0.05$. This wavelength-dependent behavior could arise from (1) the presence of multiple ground-state rotamers, each having different photodynamics, or (2) the presence of overlapping transitions to different excited electronic states, which then have different photodynamics. Both models have precedents in the literature and both models have been proposed to explain the wavelength-dependent isomerization of *t*-UCA.[27−31] It is important to resolve this issue experimentally for the following reason. Much of our

John D. Simon received his B.A in chemistry from Williams College, and his M.A. and Ph.D. from Harvard University. After a postdoctoral research position with Professor M. A. El-Sayed at UCLA, he joined the faculty at UCSD in 1985. In 1998, he accepted the position as the George B. Geller Professor in the Department of Chemistry at Duke University. His current research interests include time-resolved and spatially resolved studies of photobiological systems.

10.1021/ar970250t CCC: $19.00
Published on Web 03/01/2000

understanding of the photoreactivity of *t*-UCA comes from in vitro measurements of the molecule dissolved in buffer solutions. If the photoreactivity of *t*-UCA is due to differing ground-state rotamers, then one would need to know the rotamer populations present in both these model systems and in vivo in order to determine whether in vitro studies are relevant. If the photoreactivity is due to different excited electronic states, then in vitro studies can be directly used to analyze in vivo observations.

We have been able to unambiguously determine the origin of the wavelength-dependent isomerization behavior using pulsed-laser photoacoustic spectroscopy.[30] In our experiments, two excitation wavelengths were used, 264 and 310 nm. These two wavelengths were chosen because *t*-UCA exhibits fundamentally different photochemistry at these two wavelengths.[31] Upon excitation at 264 nm, *t*-UCA undergoes rapid intersystem crossing ($\tau < 7$ ps) to a long-lived electronically excited triplet state ($\tau > 100$ ns) that does not absorb at 310 nm. Upon excitation at 310 nm, *t*-UCA simply isomerizes ($\tau < 100$ ps) without the production of long-lived intermediate states. In pulsed-laser photoacoustic spectroscopy, the amplitude of the experimental signal is a measure of the amount of absorbed energy that is converted into heat within ~100 ns of excitation. Thus, this technique generally reveals the energetics of the primary photochemical events. Consider an experiment in which the sum of the photoacoustic signals generated by the two excitation wavelengths is compared with the signal from a two-pulse time-delayed experiment in which the 310-nm pulse overlaps the region excited by a 264-nm pulse, but arrives at the sample 9 ns after the initial excitation. The wavelength-dependent photochemical properties of *t*-UCA result in different predictions for the relationship between the sum of the photoacoustic signals for the independent excitations and the signal amplitude observed for the two-pulsed time-delayed excitation for the cases where multiple rotamers or multiple electronic states result in the observed photochemistry.

If the *t*-UCA absorption spectrum arises from the overlapping absorption of different rotamers, then the different photoreactivity observed upon excitation at 264 and 310 nm means that different rotamers dominate the absorption at these two wavelengths. In the two-pulse experiment, excitation of a *t*-UCA solution at 264 nm populates a long-lived triplet, but because the absorptions at 264 and 310 nm are due to different rotamer populations, the sample optical density at 310 nm would be unaffected by the initial excitation. Thus, the sum of the individual photoacoustic signals at 264 and 310 nm would be the same as that for the time-delayed two-pulse experiment. If the absorption spectrum of *t*-UCA arises from the overlapping absorption to more than one electronic state, then all molecules present in solution absorb at both wavelengths. In this case, excitation at 264 nm results in a decrease in the sample optical density at 310 nm. Because the triplet-state lifetime is long compared to the 9-ns time delay in the two-pulse experiment, the sum of the individual signals will be larger than the amplitude measured in the two-pulse experiment. In this case, for the sample concentration and irradiation intensities used, the two-pulse experimental signal would be ~11% smaller than the sum of the individual signals. This agrees quantitatively with our experimental result (12 ± 3%).[30] These studies establish that the seemingly structureless absorption spectrum of *t*-UCA is comprised of overlapping absorptions to different electronic states that exhibit unique photoreactivity. This conclusion means that insights into the in vivo photobiology of *t*-UCA can be inferred from in vitro measurements.

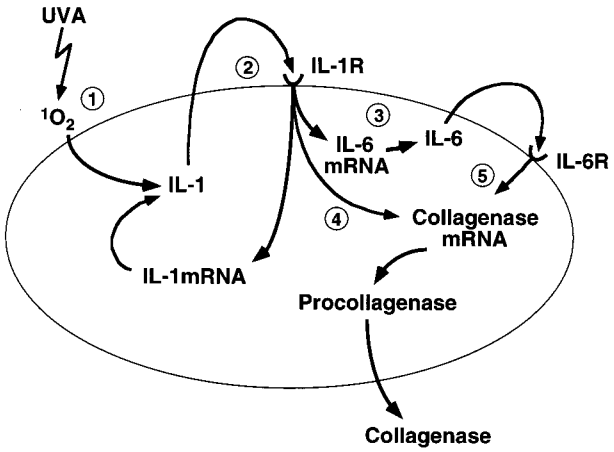

FIGURE 1. Sequence of events upon UVA irradiation of dermal fibroblasts. The UVA induction of interstitial collagenase is mediated by singlet oxygen. The sequence of events is schematically delineated by encircled numbers. IL-1R = IL-1 receptor, IL-6R = IL-6 receptor. Reprinted from ref 32 with permission. Copyright 1997.

Urocanic Acid and the Photoaging of Skin. Singlet oxygen, $O_2(^1\Delta_g)$, initiates a wide range of physiological responses and is often involved in biochemical mechanisms for the photoaging of skin. For example, from studies of UV-A irradiation of human dermal fibroblasts, Scharffetter-Kochanek and co-workers report that $O_2(^1\Delta_g)$ triggers the signaling pathway of interstitial collagenase induction.[32] Such processes ultimately lead to tissue degradation. Their mechanism for the induction of collagenase is reproduced in Figure 1.

The question at hand is what chromophore(s) in the skin causes the formation of $O_2(^1\Delta_g)$. The first step toward identifying the chromophore(s) would involve comparing the action spectrum for the photoaging of skin with the absorption spectrum of the chromophore. This approach was the basis for the immunomodulatory behavior of *t*-UCA reported by De Fabo and Noonan.[13] A quantitative comparison between photoaging action spectra and the absorption spectra of endogenous chromophores in the UV-A has remained elusive. Part of the reason such comparisons may have been slow in coming is the tendency for researchers to want to match the in vivo action spectrum with the total absorption spectrum of potential photoreceptors. This ignores the fact that the absorption spectra of molecules can be comprised of overlapping transitions, and that only one of the underlying excitations may give rise to the photoreactions that cause the observed response.

If we focus on the UV-A absorption of *t*-UCA between 310 and 380 nm, we find that the absorption cross section is small ($\epsilon < 1$ L mol^{-1} cm^{-1}). De Fabo and co-workers have reported that excitation of *t*-UCA in the wavelength range results in photoisomerization.[33] However, photoacoustic measurements show that this is not the only photochemical process that occurs in this wavelength range.[34] In addition to isomerization, excitation results in the formation of a long-lived ($>\mu$s) excited electronic state in oxygen-free solutions. The partitioning between these two processes is wavelength-dependent. This results because the absorption spectrum in this region is the superposition of two absorption bands, one that leads to isomerization, and one that leads to the formation of a long-lived reactive state that can sensitize oxygen to form $O_2(^1\Delta_g)$. Using the wavelength-dependent photoacoustic data, the efficiency spectrum for $O_2(^1\Delta_g)$ sensitization was determined.[34] The shape of the efficiency spectrum mimics the action spectrum for the photoinduced sagging of mouse skin reported by Bissett and co-workers.[4] On the basis of these results and the physiological responses initiated by $O_2(^1\Delta_g)$ (e.g., Figure 1), we proposed that UV-A excitation of *t*-UCA may initiate the photoaging process.

It is important to emphasize that we have not compared the in vivo action spectrum for photoaging with the overall absorption spectrum of *t*-UCA. Rather, the in vivo action spectrum is being compared with the efficiency for a specific chemical process ($O_2(^1\Delta_g)$ formation) that arises from a weak transition that contributes to the complicated, yet structureless absorption spectrum of *t*-UCA. At first glance, the *t*-UCA absorption spectrum would appear to be completely unrelated to any physiological response in the UV-A. However, our work shows that one must consider the possible role of weak transitions of endogenous absorbing chromophores in initiating physiological responses.

Melanin. Melanin is one of the most ubiquitous of natural pigments, and it is interesting to note that its chemical structure and biological role(s) are still subject to much debate.[35] There are two general classes of melanins: eumelanin and pheomelanin. Each type of melanin is likely to have different photodynamics. Furthermore, because the polymerization is poorly understood, it has remained impossible to assign a definitive molecular weight to melanin and to determine its precise molecular structure.[36]

It is generally believed that melanin is a photoprotective molecule that shields the skin against UV and visible radiation. The molecular mechanism of how melanin dissipates absorbed energy and thereby affords such protection is still largely unknown.[37] There is also evidence that melanin is cytotoxic at UV wavelengths.[38−42] Specifically, UV-A excitation of cultured human melanocytes demonstrated a correlation between the pheomelanin content and the amount of UV-induced single-strand breaks in the cellular DNA.[40] In vitro experiments on pheomelanin demonstrate that this pigment photoconsumes oxygen,[41] and it is reasonable to speculate that the mechanism for cellular DNA damage involves actived oxygen species. Along the same lines, exposure of eumelanin in mouse cells to UV-C radiation supports the conclusion that eumelanin also can photodamage DNA.[39] Action spectra for the generation of free radicals and the consumption of oxygen by synthetic and bovine eye eumelanin have been reported, and while this process occurs throughout the UV spectrum, the action increases with decreasing wavelength.[42] The reported action spectra for these two chemical processes and different eumelanins are identical, *but* as will be discussed below, they differ significantly from eumelanin's absorption spectrum.

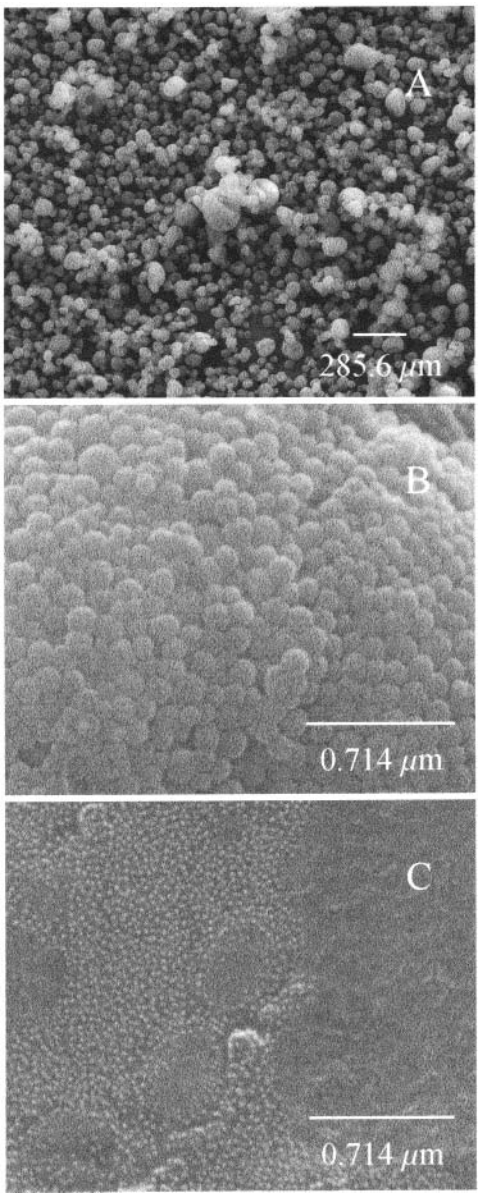

FIGURE 2. Scanning electron micrographs of melanin from *Sepia officianalis*. (A) Bulk sample. (B) An enlargement of one of the particles shown in (A). (C) Image of the 10 000 > MW > 3000 fraction, which reveals particles that range in size from 30 to 58 nm.

Size-Dependent Properties of Eumelanin. Figure 2 shows a set of images of eumelanin obtained using scanning electron microscopy (SEM). The sample in image A is a bulk sample of commercial eumelanin extracted from *Sepia officianalis* (Sigma). Image A shows that there

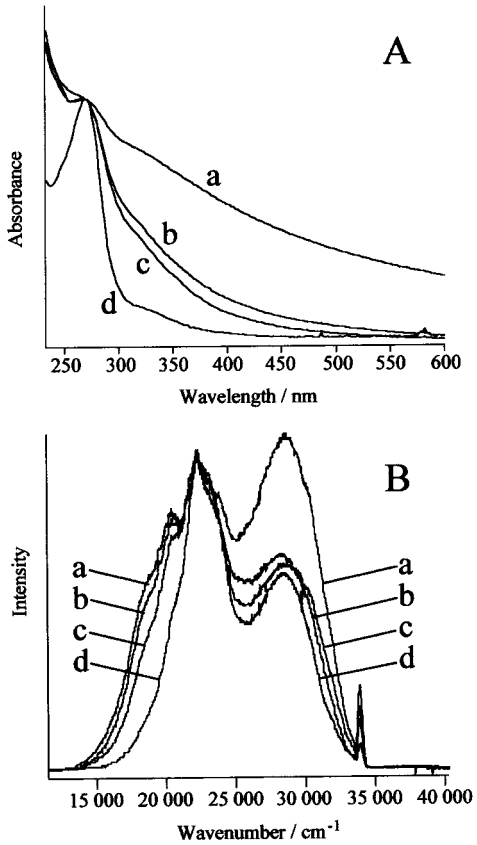

FIGURE 3. Absorption (A) and emission (λ_{ex} = 266 nm) (B) spectra for aqueous solutions of size-dependent fractions of *Sepia* eumelanin at room temperature. (a) MW > 10 000, (b) 10 000 > MW > 3000, (c) 3000 > MW > 1000, (d) MW < 1000.

is great variation in particle size and shape, and that the pigment exists as large clusters and isolated doughnut structures. These different macroscopic objects share a common substructure, shown in image B. The large particles are comprised of closely packed spherical structures of diameter 150 ± 34 nm.[43] A careful study of these images reveals small spherical objects (diameters ranging from 15 to 40 nm) that adhere to the larger sperical components. Image C shows the fraction of 10 000 > MW > 3000 (MW = molecular weight), which contains only these small particles. For the fraction of MW < 3000, a histogram of over 1000 particles gives a mean diameter of 15 nm.[44] Such small particles are the smallest particles of *Sepia* eumelanin to be isolated to date. The existence of different size melanin particles prompted us to separate eumelanin as a function of molecular weight and examine the physical and optical properties of these different aliquots.[45]

Figure 3 presents the absorption and emission spectra for four different size fractions. The absorption data (Figure 3A) have been arbitrarily normalized at 270 nm for illustration purposes. First, consider the peak at 270 nm. Eumelanin from *S. officinalis* has an associated protein coat, which cannot be fully removed in the isolation and purification process of the pigment. About 8% of the weight of the samples used in this study is protein.[46] The protein associated with these samples has been shown to contain tyrosine and phenylalanine;[47] these amino acids have an absorption peak around 270 nm. Synthetic eumelanin that is generated by the autoxidation of 3,4-dihydroxyphenylalanine lacks a protein coat and has an optical spectrum that matches the natural pigment *except* for the lack of the 270-nm component.[45] Thus, the spectral feature at 270 nm is due to absorption of light by the protein coat. The second feature worth noting is that the optical density changes in the UV-A and visible regions of the spectrum as a function of particle size. Specifically, the spectrum extends to longer wavelengths with increasing particle size. Because the molecular weight of eumelanin is not known, the absolute absorption cross section at various wavelengths cannot be determined.

There are two reasonable explanations for the size-dependent optical spectra shown in Figure 3A. First, the spectra could reflect the size-dependent absorption properties of the pigment. With increasing polymer size, it is reasonable to postulate that greater electron delocalization would occur, which would be manifested by extension of the absorption spectrum to longer wavelengths. Second, with decreasing size, particles scatter less efficiently. Thus, the trend that the optical spectrum extends to lower energies with increasing particle size could suggest that the tail of the spectrum (visible and possibly UV-A regions) is due to light scattering. Assessing the contribution of scattering from a comparison of the optical line shape to theoretical predictions has not enabled an unambiguous conclusion.

Figure 3B shows emission spectra for different particle sizes using an excitation wavelength of 266 nm. We see that the emission spectrum, like the absorption spectrum, also depends on particle size. The origin of the structure of the emission spectrum and its dependence on particle size are not known. The multiple peaks in the spectrum could correspond to emission from different chromophores that are excited by the incident light. Or, the lower energy peaks could correspond to emission from chromophores that are populated by energy transfer from an initially excited moiety of the pigment. Experiments that begin to address these issues are discussed in the next section.

Finally, photoacoustic techniques have been used to study both bulk eumelanin at various excitation wavelengths and the different size fractions using an excitation wavelength of 351 nm.[45,48] Following absorption at 527 and 400 nm, essentially all of the photon energy is released nonradiatively within a few nanoseconds of excitation,[48] in agreement with previous work.[49] At 351 nm, most of the energy was released as heat; a small amount of energy was retained (13% of the photon energy).[45] It is interesting to now ask whether the heat released upon excitation at 351 nm depends on the particle size. We find that the percentages of absorbed energy that is released as heat by the MW > 10 000, 10 000 > MW > 3000, 3000 > MW > 1000, and MW < 1000 eumelanin samples are 89 ± 7%, 91 ± 9%, 83 ± 11%, and 44 ± 3%, respectively. For the MW > 1000 samples, most of the absorbed energy is released as heat on the nanosecond or faster time scale, suggesting a negligible quantum yield for formation of long-lived intermediates. The MW < 1000 fraction, how-

ever, shows a dramatic increase in the amount of energy retained by the eumelanin particle, characteristic of the formation of a long-lived intermediate. ESR experiments on bulk samples of eumelanin from *S. officianalis* indicate the formation of electronically excited triplet states upon excitation in this wavelength region.[50] Given the inherent time scale of ESR spectroscopy, the photoacoustic data suggest that the ESR signals arise from the small particles. If we assume quantitative formation of such a reactive intermediate, then the photoacoustic measurements reveal that the energy of the triplet state of MW < 1000 eumelanin particles is ~190 kJ mol^{-1} above the ground state.

Energy Transfer within Eumelanin Aggregates. The rate at which eumelanin dissipates absorbed light energy and the mechanism by which such dissipation occurs is largely unknown. Insight into these questions can be gained from emission anisotropy measurements of eumelanin. Exciting at 335 nm and probing at 420 nm reveals that the emission depolarization dynamics is temperature-dependent, complete depolarization occurs on the ~80 ps time scale, and the initial anisotropy has a value of nearly 0.4.[51] Analysis of the temperature-dependent dynamics reveals an activation energy of 21 ± 3 kJ mol^{-1} for the depolarization process.[51] However, the depolarization dynamics were poorly fit by a single-exponential function, suggesting a more complicated process than simple first-order kinetics.

We have concluded that the rapid depolarization of the emission reflects energy-transfer processes between molecular chromophores that comprise eumelanin.[51] The observed depolarization dynamics of the emission from eumelanin requires that number of donor and acceptor sites be sufficient that the transition dipoles of the embedded "molecular emitters" cover all possible orientations in three dimensions. Unfortunately, the identity of the emitting molecular chromophores remains unknown. Insight can be gained from structural studies of eumelanins. Wide-angle X-ray diffraction measurements of synthetic eumelanin samples and STM images of monolayers of synthetic eumelanin on graphite suggest that the fundamental building block of the polymer is a three-sheet stacking structure (lateral dimension of 2.0 nm, height of 0.76 nm) consisting of 15 to 24 5,6-indolequinone residues.[52] A modeling of X-ray diffraction data of several melanins by Cheng et al. gives a similar fundamental melanin unit: a four-layer stacking of four to eight 5,6-dihydroxyindole or 5,6-indolequinone units per layer.[53]

If we take such indolequinone units to be the emitting chromophores, the above models predict that there are tens of million of such chromophores in a melanin subunit of diameter 150 nm (the mean of the particle size distribution[43]). A small fraction of these is sufficient for complete depolarization of the emission by energy transfer. Such a structural model for melanin gives rise to a large density of closely spaced excited electronic-state energies for the constituent chromophores. While energy transfer generally occurs to an acceptor site that has an electronic energy less than or equal to that of the donor, it is possible to excite acceptor with a slightly higher

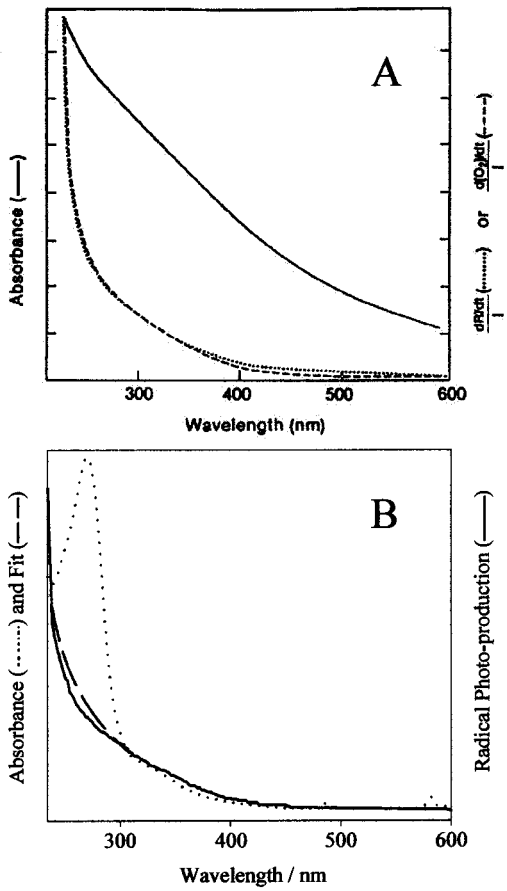

FIGURE 4. (A) Absorption spectrum of the eumelanin compared to action spectra for photoinitiated free radical production and oxygen consumption. Reprinted from ref 42 with permission. Copyright 1984. (B) Absorption spectrum of the eumelanin size fraction MW < 1000 (dotted line) compared to the average of the action spectra shown in A (solid line). The dashed line is a fit to the spectrum to approximate the absorption spectrum in the absence of protein (see text for details).

electronic energy if the energy difference is on the order of the thermal energy available. The importance of such an energy-transfer process on the depolarization dynamics increases with temperature because more potential acceptors become accessible with increased thermal energy.[54] In the case of a large density of closely spaced excited electronic-state energies, this electronic structure would manifest itself as an activated energy-transfer process, consistent with the experimental results reported.

Molecular Origin of Melanin Action Spectra—The Importance of Particle Size. Various photoreactions of melanins have been studied, and in vitro action spectra for particular chemical processes have been reported.[42] In general, as discussed above for the case of *t*-UCA, an action spectrum follows the absorption spectrum of the primary photoreceptor involved in the photochemical process. However, in the case of melanin, this relationship has not been observed. For example, Figure 4A reproduces the results of Sarna and Sealy, who compared the absorption spectrum of eumelanin to the action spectra for the photoinduced consumption of oxygen and free radical production.[42] They found that the two action spectra are essentially the same and that the action spectra are

indistinguishable for synthetic eumelanin and bovine eye melanin with and without the protein coat. Determining why these action spectra reveal a different wavelength dependence than the absorption spectrum is central to developing an understanding of the photochemical properties of this pigment and its relationship to DNA damage and skin cancer.

We now know that different-sized particles have different absorption properties,[45] so it is of interest to compare these action spectra for the photoinduced consumption of oxygen and free radical production to the data shown in Figure 3A. As shown in Figure 4B, we find that the absorption spectrum of small eumelanin particles (MW < 1000, curve d) is the only spectrum in Figure 3A that has the same shape as the action spectra for wavelengths longer than 310 nm. This comparison suggests that small eumelanin particles are responsible for this photochemical behavior. Because the wavelength dependence of the photoinduced consumption of oxygen and free radical production does not depend on the presence of protein,[42] we should compare the action and absorption spectra without regard to protein absorption (e.g., the peak at 270 nm, Figure 3A).[55] If we ignore the absorption feature centered at 270 nm and extrapolate through this region by performing a polynomial fit to the remaining part of the spectrum, then we obtain the dashed curve, which is nearly identical to the reported action spectrum. Thus, it is possible that there is quantitative agreement between these spectra in the UV-B, but we are unable to establish this because the absorption properties of the protein component have not been independently determined. Recall that photoacoustic experiments on eumelanin revealed that only the MW < 1000 particles exhibit efficient formation of a reactive intermediate. This lends further support for why we observe agreement between the MW < 1000 absorption spectrum and the action spectra for these chemical processes.

The Future. As stated in the introduction, one of the major goals of this research is to establish links between the in vitro photochemistry and the action spectra for UV-induced responses. The above discussion demonstrates that the starting point for establishing such links requires an understanding of the structure and photoreactivity of the molecules in question. In that respect, modern time-resolved and spatially-resolved spectroscopic tools can make a substantial impact.

Many important questions remain unanswered. For example, in the case of urocanic acid, once a photostationary state is achieved, the concentration of *c*-UCA exceeds that of *t*-UCA in the skin. Thus, the reactions of *c*-UCA could also contribute to the action spectra of urocanic acid in vivo. *c*-UCA generates $O_2(^1\Delta_g)$ following UV-A excitation,[30] but the action spectrum is not known. In the case of melanins, the lack of detailed knowledge about the molecular structure is clearly a major impediment to developing a detailed chemical understanding of these system. Modern mass spectrometric, imaging, and NMR techniques offer promise, and such work is currently in progress.

This work is supported by NIGMS, the North Carolina Biotechnology Center, and Duke University. I thank my co-workers Kerry Hanson, Susan Forest, Brian Nofsinger, Nicole Grynaviski, Shannon Studer-Martinez, Wai Lam, David Millar, and Leslie Eibest. I also thank Ed De Fabo, Frances Noonan, and James Grichnik for valuable discussions and insights.

References

(1) Kligman, L. H. The hairless mouse model for photoaging. *Clin. Dermatol.* **1996**, *14*, 183−195.
(2) Kligman, L. H.; Akin, F. J.; Kligman, A. M. The contributions of UVA and UVB to connective tissue damage in hairless mice. *J. Invest. Dermatol.* **1985**, *84*, 272−276.
(3) Bissett, D. L.; Hannon, D. P.; Orr, T. V. An animal model of solar-aged skin: histological, physical, and visible changes in UV-irradiated hairless mouse skin. *Photochem. Photobiol.* **1987**, *46*, 367−378.
(4) Bissett, D. L.; Hannon, D. P.; Orr, T. V. Wavelength dependence of histological, physical, and visible changes in chronically UV-irradiated hairless mouse skin. *Photochem. Photobiol.* **1989**, *57*, 763−769.
(5) Urbach, F., Ed. *Biological Responses to Ultraviolet A Radiation*; Valdenmar: Overland Park, KS, 1992.
(6) Shindo, Y.; Witt, E.;Packer, L. Antioxidant defense mechanisms in murine epidermis and dermis and their responses to ultraviolet light. *J. Invest. Dermatol.* **1993**, *100*, 260−265.
(7) Sohal, R. S.; Weindruch, R. Oxidative stress, caloric restriction, and aging. *Science* **1996**, *273*, 59−63.
(8) Vile, G. F.; Tyrrell, R. M. UVA radiation-induced oxidative damage to lipids and proteins in vitro and in human skin fibroblasts is dependent on iron and singlet oxygen. *Free Radical Biol. Med.* **1995**, *18*, 721−730.
(9) Pathak, M. A.; Carbonare, M. D. Reactive oxygen species in photoaging and biochemical studies in the amelioration of photoaging changes. In *Biological Responses to Ultraviolet A Radiation*; Urbach, F., Ed.; Valdenmar: Overland Park, KS, 1992; pp 189−207.
(10) Kvam, E.; Tyrrell, R. M. Artificial background and induced levels of oxidative base damage in DNA from human cells. *Carcinogenesis* **1997**, *18*, 2381−2383.
(11) Rigel, D. S.; Kopf, A. W.; Friedman, R. J. The rate of malignant melanoma in the United States: Are we making an impact? *J. Am Acad. Dermatol.* **1987**, *17*, 1050−1053.
(12) Pourzand, C.; Tyrell, R. M. Apoptosis, the role of oxidative stress and the example of solar UV radiation. *Photochem. Photobiol.* **1999**, *70*, 380−390.
(13) De Fabo, E. C.; Noonan, F. P. Mechanism of immune suppression by ultraviolet irradiation in vivo. Evidence for the existence of a unique photoreceptor in skin and its role in photoimmunology. *J. Exp. Med.* **1983**, *157*, 84−98.
(14) Norval, M.; Simpson, T. J.; Ross, J. A. Urocanic acid and immunosuppression. *Photochem. Photobiol.* **1989**, *50*, 267−275.
(15) Noonan, F. P.; De Fabo, E. C. Immunosuppression by ultraviolet B radiation: initiation by urocanic acid. *Immunol. Today* **1992**, *13*, 250−254.
(16) Norval, M.; McIntyre, C. R.; Simpson, T. J.; Howie, S. E.; Bardshiri, E. Quantification of urocanic acid isomers in murine skin during development and after irradiation with UVB light. *Photodermatology* **1988**, *5*, 179−186.
(17) Baden, H. P.; Pathak, M. A. The metabolism and function of urocanic acid in skin. *J. Invest. Dermatol.* **1967**, *48*, 11−17.
(18) At pH 5.6 (sweat), the tertiary nitrogen on the imidazole ring is protonated and the carboxylic acid is deprotonated. At pH 7.2 (average pH of the cell), the tertiary nitrogen on the imidazole ring is also deprotonated. Because of the asymmetry of the imidazole ring with respect to the alkene moiety, there are two possible rotamer structures. In principle, there are also two rotamers for the carboxylic group, but these are equivalent if this group is deprotonated.
(19) Morrison, H.; Avnir, D.; Bernsconi, C.; Fagan, G., Z/E photoisomerization of urocanic acid. *Photochem. Photobiol.* **1980**, *32*, 711−714.
(20) Zenisek, A.; Kral, J. A.; Hais, I. M. "Sun-screening" effect of urocanic acid. *Biochem. Biophys. Acta* **1955**, *18*, 589−591.
(21) Kurimoto, I.; Streilein, J. W. Cis-urocanic acid suppression of contact hypersensitivity is mediated via tumor necrosis factor-alpha. *J. Immunol.* **1992**, *148*, 3072−3078.
(22) Gilmour, J. W.; Norval, M. The effect of UVB irradiation, cis-urocanic acid and tumour necrosis factor-alpha on delayed hypersensitivity to herpes simplex virus. *Photodermatol. Photoimmunol. Photomed.* **1993**, *9*, 250−259.

(23) Uksila, J.; Laihia, J. K.; Jansen, C. T. Trans-urocanic acid, a natural epidermal constituent, inhibits human natural killer cell activity in vitro. *Exp. Dermatol.* **1994**, *3*, 61−65.
(24) Guymer, R. H.; Mandel, T. E. Urocanic acid as an immunosuppressant in allotransplantation in mice. *Transplantation* **1993**, *55*, 36−43.
(25) Gruner, S.; Diezel, W.; Stippe, H.; Oesterwitz, H.; Henke, W. Inhibition of skin allograft rejection and acute graft-versus-host disease by cis-urocanic acid. *J. Invest. Dermatol.* **1992**, *98*, 459−462.
(26) Mohammad, T.; Morrison, H.; HogenEsch H. Urocanic acid photochemistry and photobiology. *Photochem. Photobiol.* **1999**, *69*, 115−136.
(27) Morrison, H.; Bernasconi, C.; Pandey, G. A wavelength effect on urocanic acid E/Z photoisomerization. *Photochem. Photobiol.* **1984**, *40*, 549−550.
(28) Shukla, M. K.; Mishra, P. C. Electronic spectra, structure and photoisomerization of urocanic acid. *Spectrochim. Acta* **1994**, *51A*, 831−838.
(29) Lahti, A.; Hotokka, M.; Neuvonen, K.; Ayras, P. A theoretical study of the conformers of trans-and cis-urocanic acid. *J. Mol. Struct.* **1995**, *331*, 169−179.
(30) Hanson, K. M.; Simon, J. D. The origin of the wavelength-dependent photoreactivity of trans-urocanic acid. *Photochem. Photobiol.* **1998**, *67*, 538−540.
(31) Hanson, K. M.; Li, B.; Simon, J. D. A spectroscopic study of the epidermal ultraviolet chromophore *trans*-urocanic acid. *J. Am. Chem. Soc.* **1997**, *119*, 2715−2721.
(32) Wlaschek, M.; Wenk, J.; Brenneiseen, P.; Briviba, K.; Schwarz, A.; Sies, H.; Scharffetter-Kochanek, Singlet oxygen is an early intermediate in cytokine-dependent ultraviolet-A induction of interstitial collagenase in human dermal fibroblasts in vitro. *FEBS Lett.* **1997**, *413*, 239−242**.**
(33) Webber, L. J.; Whang, E.; De Fabo, E. C. The effects of UVA-I (340−400 nm) UVA-II (320−340 nm) and UVA-I+II on the photoisomerization of urocanic acid in vivo. *Photochem. Photobiol.* **1997**, *66*, 484−492.
(34) Hanson, K. M.; Simon, J. D. Epidermal trans-urocanic acid and the UV-A induced photoaging of the skin. *Proc. Natl. Acad. Sci. U.S.A.* **1998**, *95*, 10576−10578.
(35) Hill, H. Z. The function of melanin or six blind people examine an elephant. *BioEssays* **1992**, *14*, 49−56.
(36) Ito, S. Microanalysis of eumelanin and pheomelanin in hair and melanoma by chemical degradation and liquid chromatography. *Anal. Biochem.* **1985**, *144*, 527−536.
(37) *Melanin: Its role in human photoprotection*; Zeise, L., Chedekel, M. R., Fitzpatrick, T. B., Eds.; Valdenmar Press: Overland Park, KS, 1995.
(38) Hubbard-Smith, K.; Hill, H. Z.; Hill, G. J. Melanin both causes and prevents oxidative base damage in DNA: quantification by anti-thymine glycol antibody. *Radiat. Res.* **1992**, *130*, 160−165.
(39) Hill, H. Z.; Hill, G. J. Eumelanin causes DNA strand breaks and kills cells. *Pig. Cell Res.* **1987**, *1*, 163−170.
(40) Wenczl, E.; Van der Schans, G. P.; Roza, L.; Kolb, R. M.; Timmerman, A. J.; Smit, N. P. M.; Pavel, S.; Schothort, A. A. (Pheo)-Melanin photosensitized UVA-induced DNA damage in cultured human melanocytes, A. A. *J. Invest. Dermatol.* **1998**, *111*, 678−682.
(41) Sarna, T.; Menon, I. A.; Sealy, R. C. Photoinduced oxygen consumption in melanin systems—II. action spectra and quantum yields for pheomelanins. *Photochem. Photobiol.* **1984**, *39*, 805−809.
(42) Sarna, T.; Sealy, R. C. Free radicals from eumelanins: quantum yields and wavelength dependence. *Arch. Biochem. Biophys.* **1984**, *232*, 574−578.
(43) Zeise, L.; Murr, B. L.; Chedekel, M. R. Melanin standard method: Particle description. *Pig. Cell Res.* **1992**, *5*, 132−142.
(44) Nofsinger, J. B.; Forest, S. E.; Eibest, L.; Gold, K. A.; Simon, J. D. Probing the Building Blocks of Eumelanins Using Scanning Electron Microscopy. *Pigm. Cell. Res.*, in press.
(45) Nofsinger, J. B.; Forest, S. E.; Simon, J. D. An explanation for the disparity among the absorption and action spectra of eumelanin. *J. Phys. Chem.* **1999**, *103*,11428-11432.
(46) Chedekel, M. R.; Ahene, A. G.; Zeise, L. Melanin standard method: Empirical formula 2. *Pig. Cell Res.* **1992**, *5*, 240−246.
(47) Zeise, L.; Addison, R. B.; Chedekel, M. R. Bio-analytical studies of eumelanins. I. Characterization of melanin in the particle. *Pig. Cell Res. Suppl.* **1992**, *2*, 48−53.
(48) Forest, S. E.; Simon, J. D. Wavelength-dependent photoacoustic calorimetry study of melanin. *Photochem. Photobiol.* **1998**, *68*, 296−298.
(49) Crippa, P. R.; Viappiani, C. Photoacoustic studies of nonradiative relaxation of excited states in melanin. *Eur. Biophys. J.* **1990**, *17*, 299−305.
(50) Felix, C. C.; Hyde, J. S.; Sealy, R. C. Photoreacions of melanin: a new transient species and evidence for triplet state involvement. *Biochem. Biophys. Res. Commun.* **1979**, *88*, 456−461.
(51) Forest, S. E.; Lam, W. C.; Millar, D. P.; Nofsinger, J. B.; Simon, J. D. A model for the activated energy transfer within melanin aggregates. *J. Phys. Chem.* **2000**, *104*, 811−814.
(52) Zajac, Z. W.; Gallas, J. M.; Cheng, J.; Eisner, M.; Moss, S. C.; Alvarado-Swaisgood, A. E. The fundamental unit of synthetic melanin: a verification by tunneling microscopy and X-ray scattering results. *Biochim. Biophys. Acta* **1994**, *1199*, 271−278.
(53) Cheng, J.; Moss, S. C.; Eisner, M. X-ray characterization of melanins II. *Pig. Cell Res.* **1994**, *7*, 263−273.
(54) Parichha, T. K.; Acharyya, T. K.; Ray, R. D.; Talapatra, G. B. A Monte Carlo simulation of thermally activated spectral diffusion for an energetic and substitutionally disordered system. *J. Luminesc.* **1996**, *68*, 35−42.
(55) With decreasing particle size, the protein peak at 270 nm is more pronounced (Figure 3). One might expect the protein to cause an inner filter effect, and so it may seem suprising that the action spectrum for radical production is the same with or without the protein coat.[42] The amplitude of the 270-nm peak in the spectra shown in Figure 3 is an artifact of the sample preparation. Here, 92% of the protein is removed during the isolation process. The remainder is an impurity in the sample. These protein fragments are concentrated in the smaller fractions, explaining the observed trend in the absorption spectra. Bulk samples are used for determining action spectra, and in that case the protein makes a negligible contribution to the total optical density in a sample.[42]

AR970250T